

CL469 - Lattice Boltzmann method for fluid flows

Tutorial

on

Gravity-driven Poiseuille flow in a 2D long channel

January 14, 2025

Contents

1	Problem Statement	2
2	Analytical Solution	2
2.1	Governing Equations and Boundary conditions	2
2.2	Solution by Superposition and Variable Separation	3
3	Comparison with simulations	6

1 Problem Statement

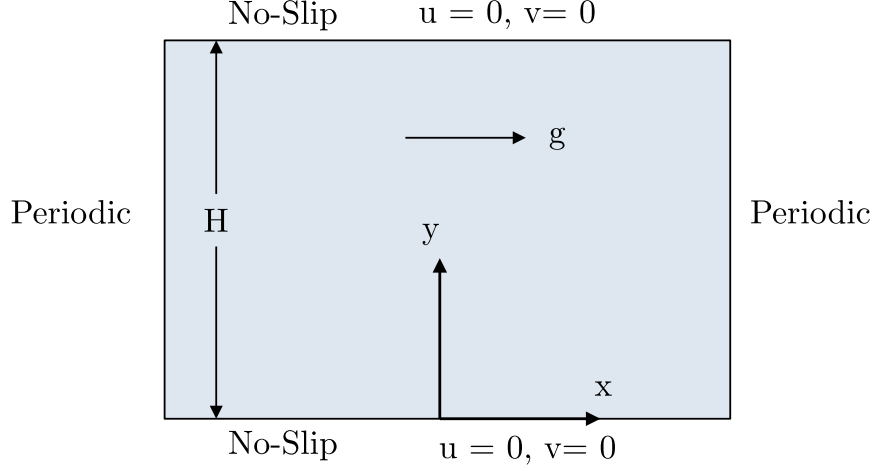


Figure 1: Schematic of a 2D channel with fluid under gravity.

Consider a 2D gravity-driven viscous flow in a long channel as shown in Fig. (1). The flow occurs in the x -direction along which gravity acts. The width of the channel in the y -direction is H . Since the situation is 2D, we neglect any variation in the z -direction. The kinematic viscosity is ν , acceleration due to gravity is $\mathbf{g} = (g_x, g_y) = (g, 0)$, density is ρ , and fluid velocity is $\mathbf{u} = (u, v)$. Considering the channel width is much smaller than the channel length and low Reynolds number, find the time-dependent analytical expression for velocity in this flow and compare it with lattice Boltzmann simulations for various resolutions.

2 Analytical Solution

2.1 Governing Equations and Boundary conditions

The governing equations for a 2D, incompressible, Newtonian fluid flow with body force are the continuity equation

$$\frac{\partial u}{\partial x} + \frac{\partial v}{\partial y} = 0, \quad (1)$$

and the Navier-Stokes equations

$$\begin{aligned} \frac{\partial u}{\partial t} + u \frac{\partial u}{\partial x} + v \frac{\partial u}{\partial y} &= -\frac{1}{\rho} \frac{\partial p}{\partial x} + \nu \left(\frac{\partial^2 u}{\partial x^2} + \frac{\partial^2 u}{\partial y^2} \right) + g_x \\ \frac{\partial v}{\partial t} + u \frac{\partial v}{\partial x} + v \frac{\partial v}{\partial y} &= -\frac{1}{\rho} \frac{\partial p}{\partial y} + \nu \left(\frac{\partial^2 v}{\partial x^2} + \frac{\partial^2 v}{\partial y^2} \right) + g_y. \end{aligned} \quad (2)$$

Since flow only happens in the x -direction and at channel walls $\mathbf{u} = \mathbf{0}$ due to no-slip and no-penetration, $v = 0$ everywhere. Furthermore, we consider an infinitely long channel

where gravity drives the flow. Hence, pressure gradients $\left(\frac{\partial p}{\partial x}, \frac{\partial p}{\partial y}\right)$ can also be neglected. Thus, Eq. (2) simplifies to

$$\frac{\partial u}{\partial t} + u \frac{\partial u}{\partial x} = \nu \left(\frac{\partial^2 u}{\partial x^2} + \frac{\partial^2 u}{\partial y^2} \right) + g. \quad (3)$$

Consider a characteristic channel length L and characteristic velocity scale U . Using non-dimensional variables

$$\bar{u} = \frac{u}{U}, \bar{y} = \frac{y}{H}, \bar{x} = \frac{x}{L} \text{ and } \bar{t} = \frac{t}{H^2/\nu} = t_\nu, \quad (4)$$

we write Eq. (3) as

$$\begin{aligned} \frac{\nu U}{H^2} \frac{\partial \bar{u}}{\partial \bar{t}} + \frac{U^2}{L} \bar{u} \frac{\partial \bar{u}}{\partial \bar{x}} &= \frac{U\nu}{H^2} \left[\left(\frac{H}{L} \right)^2 \frac{\partial^2 \bar{u}}{\partial \bar{x}^2} + \frac{\partial^2 \bar{u}}{\partial \bar{y}^2} \right] + g, \\ \text{or, } \frac{\partial \bar{u}}{\partial \bar{t}} + \frac{UH}{\nu} \bar{u} \frac{\partial \bar{u}}{\partial \bar{x}} &= \left[\left(\frac{H}{L} \right)^2 \frac{\partial^2 \bar{u}}{\partial \bar{x}^2} + \frac{\partial^2 \bar{u}}{\partial \bar{y}^2} \right] + \frac{gH^2}{U\nu}. \end{aligned} \quad (5)$$

We can define Reynolds number now as $\text{Re} = \frac{UH}{\nu}$. Thus, Eq. (5), becomes,

$$\frac{\partial \bar{u}}{\partial \bar{t}} + \text{Re} \frac{H}{L} \bar{u} \frac{\partial \bar{u}}{\partial \bar{x}} = \left[\left(\frac{H}{L} \right)^2 \frac{\partial^2 \bar{u}}{\partial \bar{x}^2} + \frac{\partial^2 \bar{u}}{\partial \bar{y}^2} \right] + \frac{gH^2}{U\nu}. \quad (6)$$

Since the channel is much longer than its width, $H \ll L$. Further, we consider low Reynolds number ($\text{Re} \ll 1$). Hence, to leading order in $\frac{H}{L}$, we can write Eq. (6) as

$$\frac{\partial \bar{u}}{\partial \bar{t}} = \frac{\partial^2 \bar{u}}{\partial \bar{y}^2} + \bar{g} + \mathcal{O}\left(\frac{H}{L}, \text{Re}\right), \quad (7)$$

where $\bar{g} = \frac{gH^2}{U\nu}$, and $\bar{u} = \bar{u}(\bar{y}, \bar{t})$.

The boundary conditions and initial conditions are

$$\bar{u}(0, \bar{t}) = 0, \bar{u}(1, \bar{t}) = 0, \text{ and } \bar{u}(\bar{y}, 0) = 0. \quad (8)$$

2.2 Solution by Superposition and Variable Separation

The simplified governing equations and boundary conditions are

$$\begin{aligned} \frac{\partial \bar{u}}{\partial \bar{t}} &= \frac{\partial^2 \bar{u}}{\partial \bar{y}^2} + \bar{g}, \\ \bar{u}(0, \bar{t}) &= 0, \\ \bar{u}(1, \bar{t}) &= 0, \\ \bar{u}(\bar{y}, 0) &= 0. \end{aligned} \quad (9)$$

Since Eq. (9) is linear, we can use the linear superposition theorem. Thus, we break $\bar{u}(\bar{y}, \bar{t})$ into a steady-state contribution $\bar{u}_{ss}(\bar{y})$ and an unsteady component $\bar{u}'(\bar{y}, \bar{t})$ as

$$\bar{u} = \bar{u}_{ss}(\bar{y}) + \bar{u}'(\bar{y}, \bar{t}). \quad (10)$$

Substituting for \bar{u} in Eq. (9), we get

$$\begin{aligned}\frac{\partial \bar{u}'}{\partial \bar{t}} &= \frac{\partial^2 \bar{u}_{ss}}{\partial \bar{y}^2} + \frac{\partial^2 \bar{u}'}{\partial \bar{y}^2} + \bar{g}, \\ \bar{u}_{ss}(0) &= 0, \bar{u}'(0, \bar{t}) = 0, \\ \bar{u}_{ss}(1) &= 0, \bar{u}'(1, \bar{t}) = 0, \\ \bar{u}'(\bar{y}, 0) &= -\bar{u}_{ss}(\bar{y}).\end{aligned}\tag{11}$$

We first solve the steady-state problem, which is

$$\begin{aligned}\frac{\partial^2 \bar{u}_{ss}}{\partial \bar{y}^2} + \bar{g} &= 0, \\ \bar{u}_{ss}(0) &= 0 \\ \bar{u}_{ss}(1) &= 0.\end{aligned}\tag{12}$$

Integrating Eq. (12) and applying the boundary conditions, we obtain the steady-state contribution as

$$\bar{u}_{ss} = \frac{\bar{g}}{2} \bar{y}(1 - \bar{y}).\tag{13}$$

One can also show that, for $\bar{y} = 1/2$, we recover the maximum velocity, which is $U = \frac{gH^2}{8\nu}$.

For the unsteady contribution, the governing equations and boundary conditions are

$$\begin{aligned}\frac{\partial \bar{u}'}{\partial \bar{t}} &= \frac{\partial^2 \bar{u}'}{\partial \bar{y}^2}, \\ \bar{u}'(0, \bar{t}) &= 0 \\ \bar{u}'(1, \bar{t}) &= 0 \\ \bar{u}'(\bar{y}, 0) &= -\bar{u}_{ss}(\bar{y}) = -\frac{\bar{g}}{2} \bar{y}(1 - \bar{y}).\end{aligned}\tag{14}$$

We don't expect a self-similar solution since we have both length and time scales. Using separation of variables a $\bar{u}'(\bar{y}, \bar{t}) = Y(\bar{y})T(\bar{t})$, we can write Eq. (14) as

$$\begin{aligned}\frac{1}{T} \frac{dT}{d\bar{t}} &= \frac{1}{Y} \frac{d^2 Y}{d\bar{y}^2} = -\lambda^2, \\ Y(0) &= Y(1) = 0,\end{aligned}\tag{15}$$

where λ is a constant. Solving Eq. (14) separately for $Y(\bar{y})$ and $T(\bar{t})$ and applying boundary conditions we obtain a general solution for $\bar{u}'(\bar{y}, \bar{t})$ as

$$\bar{u}'(\bar{y}, \bar{t}) = \sum_{n=1}^{\infty} \alpha_n \exp(-n^2 \pi^2 \bar{t}) \sin(n\pi \bar{y}),\tag{16}$$

where α_n is integration constant and $n \in \mathbb{Z}$. To determine α_n , we use the initial condition $\bar{u}'(\bar{y}, 0) = -\frac{\bar{g}}{2} \bar{y}(1 - \bar{y})$ and orthogonality condition for inner product to obtain $\alpha_n = -\frac{2\bar{g}}{n^3 \pi^3} [1 - (-1)^n]$. Thus, the unsteady component can finally be written as

$$\bar{u}'(\bar{y}, \bar{t}) = -2\bar{g} \sum_{n=1}^{\infty} \frac{[1 - (-1)^n]}{n^3 \pi^3} \exp(-n^2 \pi^2 \bar{t}) \sin(n\pi \bar{y})\tag{17}$$

Now, we can write the Non-dimensional x-component of velocity as

$$\bar{u}(\bar{y}, \bar{t}) = \frac{\bar{g}}{2} \bar{y}(1 - \bar{y}) - 2\bar{g} \sum_{n=1}^{\infty} \frac{[1 - (-1)^n]}{n^3 \pi^3} \exp(-n^2 \pi^2 \bar{t}) \sin(n\pi \bar{y}). \quad (18)$$

The solution in dimensional form can be written as

$$u(y, t) = \frac{g}{2\nu} y(H - y) - \frac{2gH^2}{\nu} \sum_{n=1}^{\infty} \frac{[1 - (-1)^n]}{n^3 \pi^3} \exp\left(-n^2 \pi^2 \frac{t\nu}{H^2}\right) \sin\left(n\pi \frac{y}{H}\right). \quad (19)$$

3 Comparison with simulations

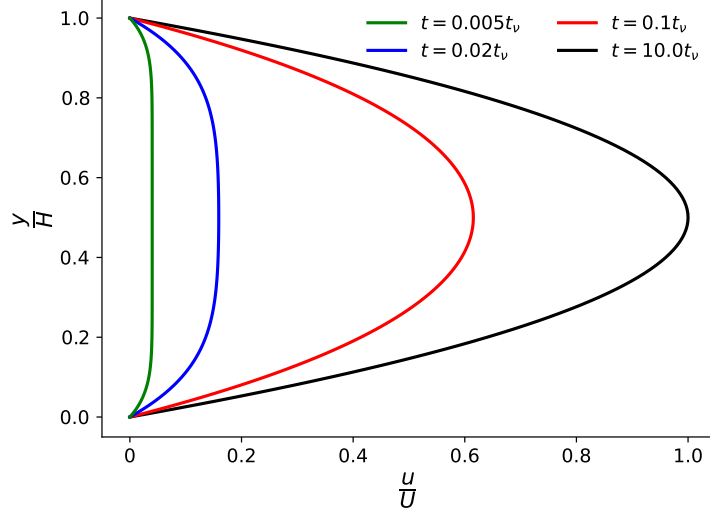


Figure 2: Analytical Velocity profiles at various time instants.

This section compares the analytical profile given in Eq. (19) with lattice Boltzmann simulations. The analytical velocity profile across the channel width at various time instants is shown in Fig. (2) considering 10 terms in the series solution. Fig. (2) clearly shows the developing flow in the channel due to gravity and the subsequent transition of the velocity profile to a parabolic nature.

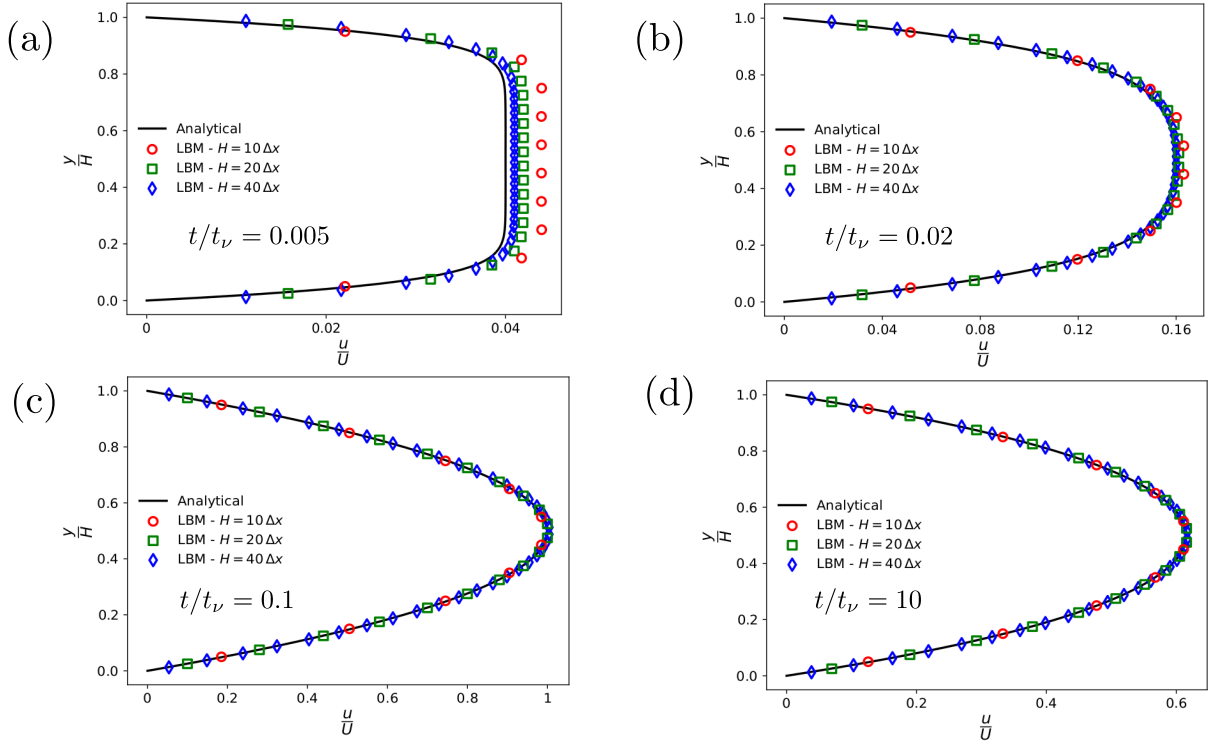


Figure 3: Velocity profiles obtained from simulations compared with analytical results for various time instants and grid resolutions.

To simulate a gravity-driven Poiseuille flow in a 2D channel, we use the weakly compressible lattice Boltzmann equation. We will discuss the details of the algorithm later in the class. We have taken $Re = 0.1$ and performed simulations for 3 resolutions, namely, $H = 10\Delta x, 20\Delta x$ and $40\Delta x$. We have considered a square computational domain of size $H \times H$. To simulate an infinitely long channel, we apply periodic boundary conditions at the left and right boundaries of the channel (see Fig. (1)). The top and bottom boundaries are modeled as walls.

Fig. (3) shows the velocity profiles obtained at various time instants. The velocity profile is well resolved at steady-state with only 10 grid points. However, the velocity gradients are not well resolved at initial time instants using fewer grid points. With increasing resolution, we see better agreement in the initial time instants.